https://doi.org/10.15407/ujpe63.5.425

A. PANTHAWAN,[1,2] T. KUMPIKA,[2] W. SROILA,[2] E. KANTARAK,[2] W. THONGPAN,[2] P. POOSEEKHEAW,[2] R. SORNPHANPEE,[2] N. JUMRUS,[2] P. SANMUANGMOON,[3] A. TUANTRANONT,[4,5] P. SINGJAI,[2,5,6] W. THONGSUWAN[2,5,6]

[1] Graduate School Chiang Mai University
(239, Huay Kaew Road, Muang, Chiang Mai 50200, Thailand)
[2] Department of Physics and Materials Science, Faculty of Science, Chiang Mai University
(239, Huay Kaew Road, Muang, Chiang Mai 50200, Thailand)
[3] Faculty of Science, Chiang Mai University
(239, Huay Kaew Road, Muang, Chiang Mai 50200, Thailand)
[4] Thailand Organic and Printed Electronics Innovation Center,
National Electronics and Computer Technology Center,
National Science and Technology Development Agency
(Klong Luang, Pathumthani, 12120, Thailand)
[5] Center of Advanced Materials of Printed Electronics and Sensors,
Materials Science Research Center, Faculty of Science, Chiang Mai University
(Chiang Mai 50200, Thailand)
[6] Materials Science Research Center, Faculty of Science, Chiang Mai University
(239, Huay Kaew Road, Muang, Chiang Mai 50200, Thailand; e-mail: wiradej.t@cmu.ac.th)

MORPHOLOGY AND PHASE TRANSFORMATION OF COPPER/ALUMINIUM OXIDE FILMS

Copper aluminium oxide ($CuAlO_2$) was successfully prepared within the single-step sparking process at the atmospheric pressure. The as-deposited films were then annealed at 400, 900, 1000, and 1100 °C in an oven. The results have shown that the annealing temperature has direct effect on the morphology, phase transformation, and optical properties. $CuAlO_2$ in the delafossite phase was formed on the annealed films at temperatures higher than 900 °C. Furthermore, the energy band gaps of the annealed films were linearly increased from 3.3 to 3.8 eV with increasing the annealing temperature from 400 to 1100 °C due to a reduction of the oxygen deficit of films at high annealing temperatures.

Keywords: sparking process, $CuAlO_2$, annealing, phase transformation.

1. Introduction

Transparent conducting oxide is one of the most advanced topics for a wide range of equipment applications and for credible wide band gap oxide semiconductors. Transparent oxides with p-type and n-type are severely limited for the development of p–n junction based devices such as transistors, transparent diodes, light emitting diodes (LEDs), and various other optoelectronic devices [1–6]. In recent years, semiconducting delafossite oxides such as copper aluminium oxide ($CuAlO_2$) have attracted much interest as p-type semiconductors due to their optical and electrical properties [8]. $CuAlO_2$ has a direct band gap in the interval 3.5–4.0 eV, while the indirect band gap is 2.0 eV [9]. Thus, $CuAlO_2$ can be used as amassing in a dye-sensitized solar cell [5]. Several methods have been used for the synthesis of $CuAlO_2$ films such as the sputtering [10–11], sol-gel [12], solution [13], pulsed laser deposition [14], chemical vapour deposition [15], and sparking [16] ones.

In this work, we prepare $CuAlO_2$ films on the quartz substrate using a single step of the sparking method without vacuum system [16]. The as-deposited films were annealed at 400, 900, 1000, and 1100 °C for 1 h. to improve their crystallinity. The morphology and structural and optical properties of the films were characterized by scanning electromicroscopy (SEM), energy dispersive x-ray (EDX), X-

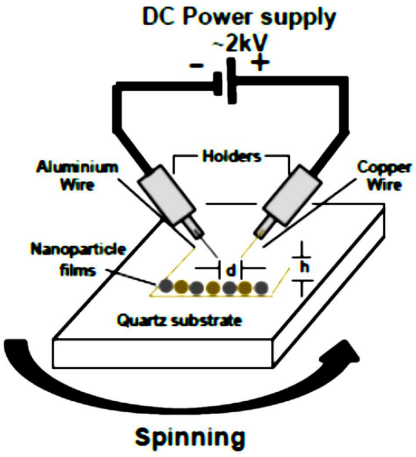

Fig. 1. Schematic diagram of a sparking apparatus

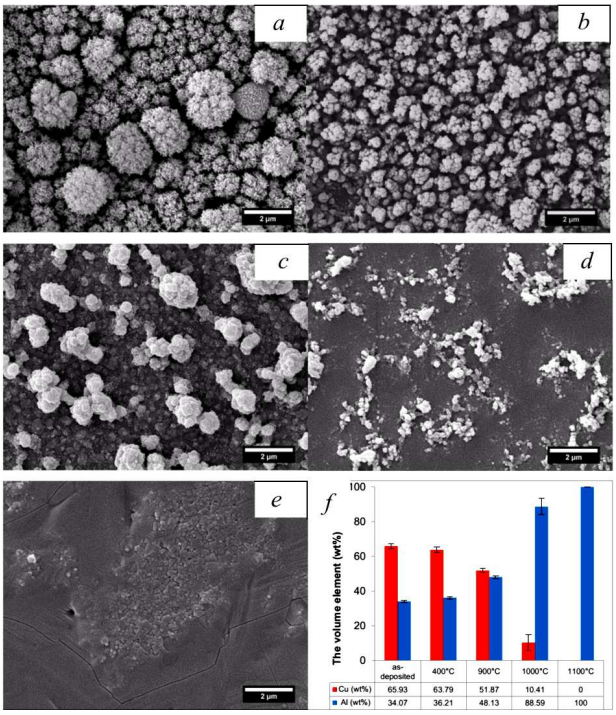

Fig. 2. SEM images of as-deposited films (*a*), the annealed films at 400 (*b*), 900 (*c*), 1000 (*d*), and 1100 °C (*e*) and their EDS (*f*)

ray diffraction (XRD), and UV/vis spectroscopy. Furthermore, the phase composition of the film surfaces was characterized using X-ray photoelectron spectroscopy (XPS). The effect of the annealing temperature on their properties will be described and discussed in what follows.

2. Experimental Details

The experiment was carried out using the sparking off Al (0.25 mm, 99.9%, SIGMA-ALDRICH Chemistry, USA) and Cu (0.58 mm, 99.9%, Advent Research Material Ltd, UK) tips with the high DC voltage of 2 kV under atmospheric pressure, as shown in Fig. 1. The tips were placed at the 1-mm spacing, while the tips were also placed above the quartz substrate at a distance of 1 mm. In the sparking process for 1 h and the deposition rate of 125 nm/min, small particles of Cu and Al, which are generated by the bombardment by electrons and ions at the two tip surfaces, were deposited on the substrate to form the films. The as-deposited films were then annealed in a furnace at 400, 900, 1000, and 1100 °C for 1 h. The film morphology was characterized by SEM (JEOL JSM300), the film components were determined by using EDX. The crystal structures and the phase composition of the films were investigated by XRD (Rigagu; CuK_α radiation with $\lambda = 0.1541862$ nm operating at 40 kV, 30 mA) and XPS (AXIS ULTRADLD, Kratos analytical, Manchester, UK). Moreover, the optical properties including the energy gap of the films can be characterized by UV/vis spectroscopy (Hitachi U-4100).

3. Results and Discussion

Fig. 2, *a*–*e* shows SEM images of the as-deposited and annealed films at 400, 900, 1000, and 1100 °C for 1 h, respectively. From the figures, it is clearly seen that the as-deposited films (Fig. 2, *a*) have a high porosity. According to the high surface energy of nanoparticles, Cu/Al nanoclusters were then agglomerated to decrease their surface energy [17]. The surface roughness and the particle sizes of the films were decreased with increasing the annealing temperature (see Fig. 2, *b*–*e*). When the films are annealed at 900 and 1000 °C, it is seen that some of Al particles are melted, because the melting temperature of Al is lower than 900 °C [18]. When the films are annealed at 1100 °C, Cu/Al particles are totally melted since the temperature was higher than the melting point of copper [18]. The weight % of Cu/Al on the films is shown in Fig. 2, *f*. It is found that the weight % of Cu decreases, while the weight % of Al increases, as the annealing temperature increases. This is because the melting temperature of Al lower than that of Cu leads

to the coverage on Cu particles at the high annealing temperature.

Figure 3 shows XRD patterns of the as-deposited films and films annealed at various temperatures for 1 h. From the figure, no significant peak is observed at the annealing temperature lower 400 °C. At the annealing temperature of 900 °C, the peaks were observed at 35.6° and 38.9°, which correspond to CuO [19], while the peak at 36.9° is related to $CuAl_2O_4$ [20]. After the annealing at more that 900 °C, the peaks are clearly observed at 21.6° and 35.8°, which confirms that the film is $CuAlO_2$ [21].

The $CuAlO_2$ film annealed at 1100 °C were studied by XPS spectra, as shown in Fig. 4. From the figure, we see that all strong peaks of Cu, Al, and O correspond to the state of $CuAlO_2$. That is, the main peaks of Cu 2*p* were observed at the binding energies of 933.2 eV and 952.9 eV, which correspond to Cu $2p_{3/2}$ and the spin orbital Cu $2p_{1/2}$ (see Fig. 4, *a*) [22]. However, the states of CuO are remained at 935.0 eV and 953.9 eV, while the states of $CuAl_2O_4$ are also remained at 934.6 eV and 952.6 eV [24]. Figure 4, *b* shows the Al 2*p* (Al^{3+}) peak at 74.5 eV, which corresponds to Al^{+3}–O^{-2} bonds of $CuAlO_2$ [22], whereas the peak at 74.7 eV corresponds to $CuAl_2O_4$ [25]. Figure 4, *c* shows the main peak at 532.6 eV of O 1*s*, which corresponds to O^{2-}–Cu^{+1} [22]. The binding energy at 531.4 eV corresponds to O^{-2}–Al^{+3}. However, the peak at 533.8 eV was observed due to the aggregation of $(O_2)^{2-}$ peroxo species [23]. Thus, the XRD results show not only the peak of $CuAlO_2$ (Fig. 3), but also confirm the presence of $CuAlO_2$ observed on the films by XPS spectra.

The optical transmission spectra of the as-deposited and annealed films at 400, 900, 1000, and 1100 °C in for 1 h have shown in Fig. 5. The transmission of the as-deposited and annealed films at 400 °C rapidly decreases from 90 to 20% with decreasing the wavelength from 1000 to 200 nm. It might be from the absorption and scattering of the amorphous structure [26]. If the annealing temperature is higher than 900 °C, the transmission slightly decreases with decreasing the wavelength from 1000 to 300 nm. The transmission then rapidly decreases for the wavelengths lower than 300 nm due to the formation of the $CuAlO_2$ phase on the films [27].

The energy band gap (E_g) values, which can be indicated using the transmission spectra (see Fig. 5),

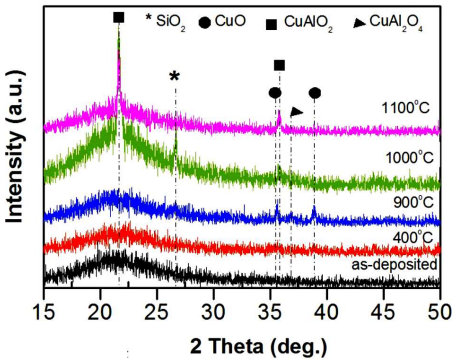

Fig. 3. XRD patterns of the Cu/Al films at various annealing temperatures

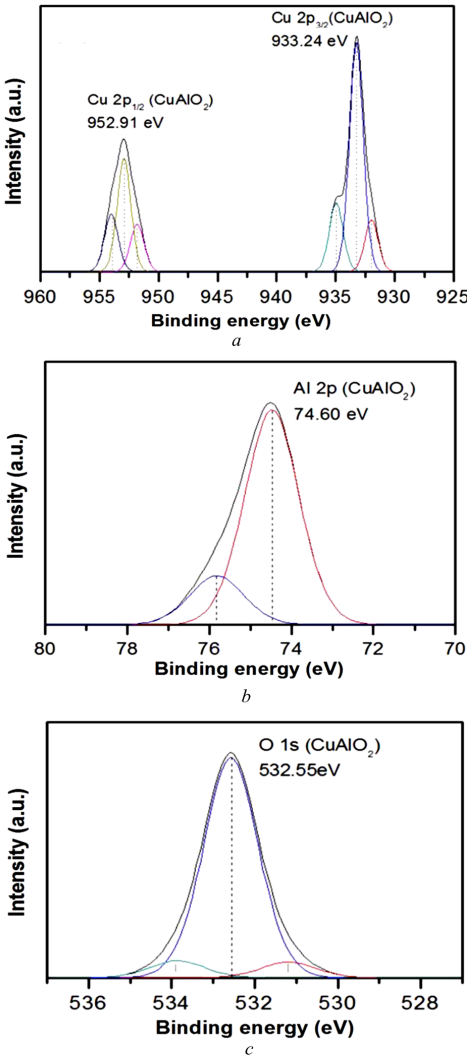

Fig. 4. XPS spectra of Cu 2*p* (*a*), Al 2*p* (*b*) and O 1*s* (*c*); the films were annealed at 1100 °C for 1 h

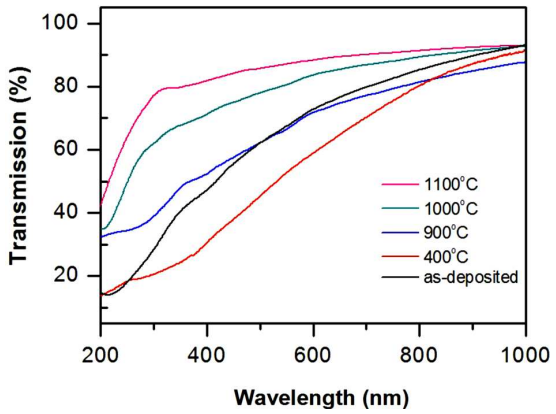

Fig. 5. UV-Vis transmission spectra of the as-deposited and annealed films at various annealing temperatures

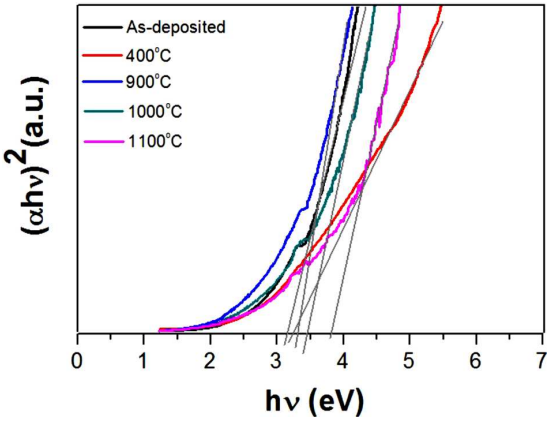

Fig. 6. Plot of $(\alpha h\upsilon)^2$ versus the photon energy for the determination of the as-deposited and annealed films at various annealing temperatures

are shown in Fig. 6. The Tauc plot is used to generate the optical band gap (E_g) and can be written as follows [28]:

$$\alpha h\upsilon = A(h\upsilon - E_g)^Z, \tag{1}$$

$$\alpha = \frac{1}{t}\ln\left(\frac{1}{T}\right). \tag{2}$$

Here, α is an optical absorption coefficient of the films which can be calculated using relation (2) [29, 37], A is a constant dependent on the photon energy, $h\upsilon$ is the photon energy, and T is the transmittance. The exponential Z is 2 or $\frac{1}{2}$ for the indirect or direct allowed transition. However, the assuming α without the film thickness value (t) was slightly different [35, 36]. Thus, the optical band gap (E_g) can be determined using a plot of $(\ln(1/T)^* h\upsilon)^2$ against the energy $h\upsilon$, as shown in Fig. 6. From the figure, the (E_g) of the as-deposited films was 3.2 eV, while the annealed films at 400, 900, 1000, and 1100 °C were 3.3, 3.4, 3.5, and 3.8 eV respectively. We note that E_g increases with the annealing temperature due to the formation of $CuAlO_2$ at high temperatures [33]. This is because the increasing of the band gap is required to reduce the oxygen deficit [9], which in good agreement with all of the above-mentioned researchers [30–34].

4. Conclusions

Cu/Al composited films were deposited on the quartz substrate by the single-step sparking method at the atmospheric pressure. The morphology and structural and optical properties of the annealed films at various temperatures are totally different from the as-deposited films. Furthermore, XRD and XPS spectra have confirmed that $CuAlO_2$ in the delafossite phase was formed on the films annealed at high temperatures.

The authors would like to thank the financial support from Thailand Graduate Institute of Science and Technology (TGIST) (SCA-CO-2560-4484-TH, TG-44-10-60-023D), National Science and Technology Development Agency (NSTDA), Center of Advanced Materials for Printed Electronics and Sensors, Materials Science Research Center, the National Research University (NRU) Project under Thailand's office of the Commission on Higher Education (CHE), the Thailand Research Fund (TRF), Center of Excellence in Advanced Materials for Printed Electronics and Sensors (CMU-NECTECH), and the Graduate School Department of Physics and Materials Science, Faculty of Science, Chiang Mai University GSCMU).

1. M. Miclaua, N. Miclaub, R. Banicaa *et al.* Effect of polymorphism on photovoltaic performance of $CuAlO_2$ delafossite nanomaterials for *p*-type dye-sensitized solar cells application. *Materials Today: Proceedings* **4**, 6975 (2017).
2. S. Pantian, R. Sakdanuphab, A. Sakulkalavek. Enhancing the electrical conductivity and thermoelectric figure of merit of the *p*-type delafossite $CuAlO_2$ by Ag_2O addition. *Current Appl. Phys.* **17**, 1264-127 (2017).

3. L. Hao, N. Feng, Y. Jinc *et al.* $CuAlO_2$ thermoelectric compacts by SPS and thermoelectric performance improvement by orientation control. *Ceramics International* **34**, 12154 (2017).
4. K. Vojisavljevic, B. Malic, M. Senna *et al.* Solid state synthesis of nano-boehmite-derived $CuAlO_2$ powder and processing of the ceramics. *J. Europ. Ceramic Society* **33**, 3231 (2013).
5. T. Suriwong, T. Thongtem, S.Thongtem. $CuAlO_2$ powder dispersed in composite gel electrolyte for application in quasi-solid state dye-sensitized solar cells. *Mater. Sci. Semicond. Proc.* **39**, 348 (2015).
6. A.N. Banerjee, S. Nandy, C.K. Ghosh *et al.* Fabrication and characterization of all-oxide heterojunction p-$CuAlO_{2+x}$/n-$Zn_{1-x}Al_xO$ transparent diode for potential application in "invisible electronics". *Thin Solid Films* **515**, 7324 (2007).
7. I.Y.Y. Bu. Optoelectronic properties of novel amorphous $CuAlO_2$/ZnO NWs based heterojunction. *Superlatt. Microstruct.* **60**, 160 (2013).
8. C.-L. Jiang, Q.J. Liu, F.S. Liu *et al.* Stability and electronic properties of $CuAlO_2$ (1120) surfaces. *Current Appl. Phys.* **17**, 126 (2017)
9. K.R. Murali, M. Balasubramanian. Properties of $CuAlO_2$ thin films deposited by polyacrylamide gel route. *Mater. Sci. Semicond. Process.* **16**, 38 (2013).
10. R.E. Stauber, J.D. Perkins, P.A. Parilla *et al.* Thin film growth of transparent p-type $CuAlO_2$. *Electrochem. Solid-State Lett.* **2**, 654 (1999).
11. W. Lan, M. Zhang, G.B. Dong *et al.* The effect of oxygen on the properties of transparent conducting Cu–O thin films deposited by rf magnetron sputtering. *Mater. Sci. Engin. B* **52**, 75 (2009).
12. C.K. Ghosh, S.R. Popuri, T.U. Mahesh *et al.* Preparation of nanocrystalline $CuAlO_2$ through sol-gel route. *J. Sol-Gel Sci. Technol.* **139**, 155 (2007).
13. K. Tonooka, K. Shimokawa, O. Nishimura. Properties of copper-aluminum oxide films prepared by solution methods. *Thin Solid Films* **411**, 129 (2002).
14. H. Kawazoe, M. Yasukawa, H. Hyodo *et al.* P-type electrical conduction in transparent thin films of $CuAlO_2$. *Nature* **389**, 939 (1997).
15. S.H. Chiu, J.C.A. Huang. Characterization of p-type $CuAlO_2$ thin films grown by chemical solution deposition. *Surface & Coatings Technology* **231**, 239 (2013).
16. Y. Chuminjak, S. Daothong, A. Kuntarug *et al.* High-performance electrochemical energy storage electrodes based on nickel oxide-coated nickel foam prepared by sparking method. *Electrochimica Acta* **238**, 298 (2017).
17. T. Ghosh, B. Satpati. Role of oxygen in wetting of copper nanoparticles on silicon surfaces at elevated temperature. *Beilstein J. Nanotechnol.* **8**, 425 (2017).
18. Y. Tian, C. Hang, C. Wang *et al.* Evolution of Cu/Al intermetallic compounds in the copper bump bonds during aging process. *Conference on Electronic Packaging Technology, 2007.*
19. P. Niggli. Die kristallstruktur einiger oxyde I. *Z. Kristallogr., Kristallgeom., Kristallphys., Kristallchem.* **57**, 253 (1922).
20. J.C. Lambert, W. Eysel. Mineralogical-Petrograph. Institute, Universitat Heidelberg, Germany, ICDD Grant-in-Aid (1980).
21. W. Gessner. Über die Modifikationen der "Aluminate" $Me^{I}AlO_2$ des einwertigen Ag, Cu und Tl. *Z. Anorg. Allg. Chem.* **352**, 145 (1967).
22. S. Liu, Z.Wu, Y. Zhang *et al.* Strong temperature-dependent crystallization, phase transition, optical and electrical characteristics of p-type $CuAlO_2$ thin films. *Phys. Chem. Chem. Phys.* **17**, 557 (2015).
23. J. Luo, Y.J. Lin, H.C. Hung *et al.* Tuning the formation of p-type defects by peroxidation of $CuAlO_2$ films. *J. Appl. Phys.* **114**, 033712 (2013).
24. F. Parmigiani, G. Pacchioni, F. Illas *et al.* Studies of the Cu-O bond in cupric oxide by X-ray photoelectron spectroscopy and ab initio electronic structure models. *J. Electron Spectrosc. Relat. Phenom.* **59**, 255 (1992).
25. J.C. Klein, C.P. Li, D.M. Hercules *et al.* Decomposition of copper compounds in X-ray photoelectron spectrometers. *Appl. Spectrosc.* **38**, 729 (1984).
26. A.S. Reddy, P.S. Reddy, S. Uthanna *et al.* Characterization of $CuAlO_2$ films prepared by dc reactive magnetron sputtering. *J. Mater. Sci.: Mater. Electron.* **17**, 615 (2006).
27. Y.J. Zhang, Z.T. Liu, D.Y. Zang *et al.* Effect of annealing temperature on the microstructure and optical-electrical properties of Cu–O thin films. *J. Phys. Chem. Solids* **74**, 1672 (2013).
28. H. Hiramatsu, W.S. Seo, K. Koumoto. Electrical and optical properties of radiofrequency-sputtered thin films of $(ZnO)_5In_2O_3$. *Chem. Mater.* **10**, 3033 (1998).
29. F. Demichelis, G. Kaniadakis, A. Tagliaferro *et al.* New approach to optical analysis of absorbing thin solid films. *Appl. Opt.* **26**, 1737 (1987).
30. G. Dong, M. Zhang, X. Zhao *et al.* Influence of working gas pressure on structure and properties of $CuAlO_2$ films. *J. Cryst. Growth.* **311**, 1256 (2009).
31. H. Luo, M. Jain, T.M. McCleskey *et al.* Optical and structural properties of single phase epitaxial p-type transparent oxide thin films. *Adv. Mater.* **19**, 3604 (2007).
32. C. Bouzidi, H. Bouzouita, A. Timoumi *et al.* Fabrication and characterization of $CuAlO_2$ transparent thin films prepared by spray technique. *Mater. Sci. Eng. B* **118**, 259 (2005).
33. W. Lan, W. L. Cao, M. Zhang *et al.* Annealing effect on the structural, optical, and electrical properties of $CuAlO_2$

films deposited by magnetron sputtering. *J. Mater. Sci.* **44**, 1594 (2009).

34. S.Iping, Z. Lockman, S.D. Hutaglung *et al.* Formation of $CuAlO_2$ Film by Ultrasonic Spray Pyrolysis. *Mater. Sci. Eng.* **18**, 082022 (2011).
35. Q. Wang, G. Wang, J. Jie *et al.* Annealing effects on optical properties of ZnO films fabricated by cathodic electrodepostion. *Thin Solid Films* **44**, 61 (200).
36. T. Kumpika, W. Thongsuwan, P. Singjai. Atomic force microscopy imaging of ZnO nanodots deposited on quartz by sparking off different tip shapes. *Surf. Interface Anal.* **39**, 58 (2007).
37. J. Tauc. Optical properties and electronic structure of amorphous Ge and Si. *Materials Research Bulletin* **3**, 37 (1968).

Received 28.12.17

А. Пантаван, Т. Кумпіка, В. Сроіла,
Е. Кантарак, В. Тонгпан, П. Пусіхів,
Р. Сорнфанрі, Н. Джумрус, П. Санмуанмун,
А. Туантранонт, П. Синджан, В. Тонгсуван

МОРФОЛОГІЯ І ФАЗОВЕ
ПЕРЕТВОРЕННЯ ПЛІВОК ОКИСУ МІДІ/АЛЮМІНІЮ

Р е з ю м е

Одностадійним електроіскровим методом при атмосферному тиску отримано окис міді і алюмінію $CuAlO_2$. Тільки що виготовлені плівки відпалені в печі при 400, 900, 1000 і 1100 °C. Результати показали, що морфологія, фазове перетворення і оптичні властивості залежать від температури відпалу. $CuAlO_2$ у фазі делафоссіта утворюється на відпалених плівках за температурою вище 900 °C. Ширина забороненої зони відпалених плівок лінійно зростає від 3,3 до 3,8 еВ із збільшенням температури відпалу від 400 до 1100 °C завдяки зменшенню дефіциту кисню при високих температурах відпалу.